chemosensors

Article

Enhanced Visible Light Absorption and Photophysical Features of Novel Isomeric Magnesium Phthalocyaninates with Cyanophenoxy Substitution

Dmitry Erzunov, Svetlana Tonkova, Anastasia Belikova and Arthur Vashurin *

Department of Inorganic Chemistry, Ivanovo State University of Chemistry and Technology, Ivanovo 153000, Russia
* Correspondence: vashurin@isuct.ru

Abstract: Novel metal-free and Mg(II) [3/4-(3,4-dicyanophenoxy)phenoxy]-substituted phthalocyanines were obtained and characterized using NMR, IR, UV-vis spectroscopy, and mass spectrometry. This substitution provided compounds with good solubility in organic media, and thus their spectroscopic and fluorescent properties were studied. The formation of the investigated phthalocyanine complexes with central magnesium ions led to the stabilization of macrocyclic molecules in solution, preventing aggregation through specific and universal solvation. From meta-substitution to para-substitution, insignificant spectroscopic changes were observed. The complexes exhibited higher values of molar light absorption coefficients and fluorescence quantum yields (up to 55%) compared to ligands. The efficiency of both the fluorescence-quenching and singlet oxygen generation processes in the case of magnesium [3/4-(3,4-dicyanophenoxy)phenoxy]phthalocyaninates was found to exceed that of the unsubstituted zinc phthalocyaninate, which suggests the potential applicability of these compounds as PDT sensitizers.

Keywords: phthalocyanines; complexes; photochemistry; singlet oxygen

Citation: Erzunov, D.; Tonkova, S.; Belikova, A.; Vashurin, A. Enhanced Visible Light Absorption and Photophysical Features of Novel Isomeric Magnesium Phthalocyaninates with Cyanophenoxy Substitution. *Chemosensors* **2022**, *10*, 503. https://doi.org/10.3390/chemosensors10120503

Academic Editors: Jianliang Shen, Ji-Ting Hou and Xiaojun He

Received: 5 November 2022
Accepted: 25 November 2022
Published: 28 November 2022

1. Introduction

Phthalocyanines (Pcs) have a macrocyclic aromatic structure conjugated by 18 π-electrons [1]. Therefore, this class of compounds has valuable optical, thermal, and electrochemical properties [2–4]. Phthalocyanines have been used in many technological and medical applications [5,6], such as catalysts, light-emitting diodes, biological imaging, gas sensors, dyes, and pigments. Additionally, these compounds are suitable photosensitizers for photodynamic therapy (PDT) applications, with their high absorption in the visible region, absence of toxicity in the dark, high stability in solutions, high singlet oxygen yield, and high selectivity for high-quality tissues [7–9]. In addition, the phthalocyanine ring can exhibit redox properties due to the high level of π-electron delocalization [10,11].

Phthalocyanines can be modified in various ways by adding substituents at their non-peripheral and peripheral positions. Phthalocyanines have poor solubility in organic solvents and form aggregates, which affects their use in many fields. The solubility of compounds of this class can be augmented by the introduction of substituents such as phenoxy, alkyl, alkoxy and bulky or long-chain groups at peripheral and non-peripheral positions to the macrocycle core [12–17]. The combination of such structures makes it possible to obtain molecular assemblies with the necessary useful properties and, at the same time, to negate the adverse factors affecting their use, such as molecular aggregation [18–20].

Fluorescence is an important characteristic of phthalocyanines and has recently found many applications in the field of biomedical sensors and fluorescence imaging. In recent years, many photosensitizers for PDT based on phthalocyanines with luminescent-active metals, such as magnesium, have been obtained and studied. However, most macrocycles

absorb and emit in the far red region of the light spectrum, and only a limited range of structures possess absorption in the near infrared region [21,22].

The structure of the introduced ligand has a significant effect on the photophysical properties of the complex and can both promote and inhibit the processes of energy transfer between the organic fragment and the complexing atom. Thus, the key task is to search for structures with suitable electronic and steric parameters that are capable of effectively realizing the entire energy potential of the central metal ion.

As mentioned earlier, the course of aggregation processes in solution strongly affects the properties of the complexes. It leads to a decrease in the intensity of light absorption and red or blue shifts in their maxima; the screening/clogging of the coordination center of the molecule, followed by the impossibility of extra-coordination and a significant decrease in catalytic activity; a significant decrease in the quantum yields of fluorescence and singlet oxygen; etc. [23–28]. Thus, the study of their spectroscopic and aggregation properties is a prerequisite for working with these compounds, and the preparation of structures resistant to aggregation makes it possible to obtain highly efficient materials for various spheres of human life.

The obtainment of phthalocyaninates with functional substituents, especially cyano groups, entails a number of difficulties that limit the possibility of their synthesis. The main problem is the occurrence of polymerization processes, leading to the formation of oligomers and polymers of various structures based on phthalocyaninates. At present, the preparation and study of monomeric cyano-substituted phthalocyaninates has been described in a limited number of works [29,30]. Despite this, phthalocyanines with terminal cyano groups in the peripheral and non-peripheral positions of the macroring may exhibit outstanding spectroscopic, catalytic, chelating, and other properties due to the possibility of further modifying the structure of the macroheterocyclic molecule. Thus, the introduction of additional fragments and coordination centers, or the conjugation of macro fragments of another compound class with the formation of complex supramolecular structures, and the further possibility of their functionalization to obtain hybrid materials with useful application properties have become possible.

Earlier, we studied complexes of *d*-metals with the described ligands and showed the fundamental differences and advantages of this type of substitution [26,31]. It was shown that the presence of aromatic fragments led to compounds with good solubility in most organic solvents, and their massiveness was compensated for by the presence of oxygen bridges, which provided the molecules with flexibility in space, thereby contributing to aggregation stability. The presence of terminal cyano groups, however, opens up access for the further simple modification of the structures. This work presents the synthesis of magnesium phthalocyanine complexes with [3/4-(3,4-dicyanophenoxy)phenoxy]-peripheral substitution and their metal-free analogues. It was assumed that the results obtained would contribute to the fundamental aspects of the chemistry of photoactive compounds, especially of the macroheterocyclic type, and would find potential practical application as highly effective photosensitizing agents for the diagnosis and treatment of tumor diseases.

2. Materials and Methods

2.1. Equipment

Elemental analysis was carried out on a CHNS-OFlashEA 1112 series analyzer (Thermo Quest, Milan, Italy). Electronic absorption (UV-vis) spectra were recorded using UNICO2800 (United Products and Instruments, Dayton, NJ, USA) and AVANTES (Avantes, Louisville, KY, USA) spectrophotometers in the region of 190–1100 nm utilizing quartz cuvettes of 1 cm optical path length. IR spectra were obtained on an IRAffinity-1S spectrometer (Shimadzu, Kyoto, Japan) at wavenumbers from 450 to 4500 cm^{-1}. NMR spectroscopy was conducted on a Bruker AVANCE 500 (Bruker, Bremen, Germany) registering ^{1}H nuclear at 500 MHz in $CDCl_3$. TMS was used as an internal standard. MALDI-TOF mass spectra were obtained by means of the time-of-flight Simadzu Axima Confidence mass spectrometer (Shimadzu, London, UK). Samples of approximately 10^{-3} mol/L concentration were

stored in tetrahydrofuran, and CHCA (alpha-cyano-4-hydrohycinnamic acid) was used as a matrix.

The purification of the metal phthalocyaninates was performed through column (on silica gel 60, 200–400 mesh) and gel permeation (on Bio-Beads S-X1) chromatography, with the process controlled by TLC.

2.2. Materials

4-nitrophthalonitrile (99%, Sigma-Aldrich, St. Louis, MO, USA); chloroform ($CHCl_3$) (99%); ethyl alcohol (99%); acetone (99%); dimethylformamide (DMF) (99%); hydrochloric acid (33%); resorcinol (98%); benzoquinone (99%); deuterated dimethylsulfoxide (DMSO-d_6) (99.9%); deuterated chloroform ($CDCl_3$) (99.9%); *iso*-amyl alcohol (98%); octanol (99%); and quinoline (99%) were applied without additional purification. Potassium carbonate and acetate of lanthanides were dehydrated immediately before the experiments.

2.3. Methods

2.3.1. Fluorescence Quantum Yield (Φ_x) and Lifetime (τ_f) Determination

Fluorescence is the emission of a photon at a certain wavelength as an electron in the excited state returns to the ground state. The fluorescence lifetime is closely connected to the fluorescence quantum yield and denotes the average time for which a molecule stays in its excited state before fluorescing. The fluorescence quantum yields were determined by the comparative method with a reference solution of unsubstituted zinc phthalocyaninate (ZnPc) in pyridine (Φ_s(ZnPc) = 0.3, λ_{ex} = 610 nm) [27].

The fluorescence quantum yield (Φ_x) was calculated by the formula:

$$\Phi_x = \frac{A_s F_x n_x^2}{A_x F_s n_s^2} \cdot \Phi_s \quad (1)$$

where Φ_x and Φ_s are the fluorescence quantum yields of the test and reference substances, respectively; A_x and A_s are the optical densities at the fluorescence excitation wavelength of the test and reference substances, respectively; F_x and F_s are the areas under the fluorescence peaks of the test and reference substances, respectively; and n_x and n_s are the refractory indexes of the solvents used for the test and reference substances, respectively.

The fluorescence lifetime (τ_f) is the average time for which a molecule stays in its excited state before fluorescence, and this value is directly related to that of Φ_x. The fluorescence lifetimes were calculated using the Strickler-Berg Equation (2). The fluorescence lifetimes of the obtained compounds were determined by the time-correlated single-photon counting (TCSPC) method. In all cases, the decay curve was described by a mono-exponential function. The object of comparison was a solution of LUDOX (nano-sized silica particles) in H_2O.

$$\Phi_x = \frac{\tau_f}{\tau_0} \quad (2)$$

where τ_0 is the natural radiative lifetime.

2.3.2. Fluorescence Quenching Studies

Fluorescence quenching was determined by adding a quencher (benzoquinone (BQ)) at different concentrations to a phthalocyanine solution at a constant concentration. Furthermore, according to the Stern-Volmer Equation (3), the values of the corresponding constants (K_{SV}) were determined based on the value of the slope of the I_0/I dependence on BQ:

$$\frac{I_0}{I} = 1 + K_{SV}[BQ] \quad (3)$$

2.3.3. Singlet Oxygen Quantum Yield (Φ_Δ) Determination

The quantum yields of singlet oxygen were determined using the comparative method (ZnPc in THF was chosen as the object of comparison) using diphenylisobenzofuran (DPBF)

as a trap. A solution of DPBF in THF (~5 × 10^{-5} M) was placed in a quartz cuvette, and oxygen was passed through the solution for 1 min. Next, a concentrated sample of the phthalocyanine solution was added to the vessel so that the absorption maximum of the *Q*-band did not exceed 0.1 (and had the same value throughout the entire series of experiments). The resulting solution was irradiated with a xenon lamp for fixed periods of time, and the electronic absorption spectrum of the solution was recorded at each stage. During the experiment, a decrease in the DPBF band (415 nm) was observed. The quantum yield of singlet oxygen was calculated by the following formula:

$$\Phi_{\Delta}^{S} = \Phi_{\Delta}^{R} \frac{k^{S} I_{aT}^{R}}{k^{R} I_{aT}^{S}} \quad (4)$$

where k is the slope of $\ln(A_0/A_t)$ versus irradiation time; A_0 and A_t are the absorption of DPBF at the initial time and after irradiation at time t, respectively; I_{aT} is the total amount of light absorbed by the compound, defined as the sum of the intensity of absorption in the range of 523–850 nm (light at lower wavelengths was not absorbed due to the use of a filter); and *R* and *S* indicate the reference and sample, respectively.

2.4. Synthesis of Substituted Phthalodinitriles

Compounds **2**–**3** were obtained according to the modified method described in a previous work [25].

Resorcinol (in the case of compound **2**) or hydroquinone (in the case of compound **3**) (0.64 g, 5.76 mmol) were dissolved in 200 mL of dry DMF with K_2CO_3 (1.19 g, 8.64 mmol) and then refluxed for 1 h. Next, extra portions of K_2CO_3 (1.78 g, 13.06 mmol) and 4-nitrophthalonitrile (0.49 g, 2.88 mmol) were added, and the reaction mixture was stirred for another 7 h. At the end of the reaction, the mixture was poured into 300 mL of 0.1 M NaOH aqueous solution. The resulting precipitates were filtered off and consecutively washed with deionized water, 0.1 M NaOH aqueous solution, and deionized water again until a neutral pH was reached. The obtained coarse crude crystals were recrystallized using ethanol to remove any residuals. The pure product was obtained as a light-yellow powder that was soluble in chloroform, ethanol, and acetone.

2.4.1. 4,4′-[1,3-Phenylenebis(oxy)]diphthalonitrile (**2**)

Yield: 0.68 g (65%) mp 190 °C. FT-IR: ν_{max}, cm^{-1} 3080, 2920, 2850 (C_{ar}–H); 2230 (C≡N); 1600, 1480 (C_{ar}=C_{ar}); 1240 (Ar–O–Ar). ^{1}H NMR (500 MHz, $CDCl_3$): δ, ppm 7.76 (dd, 2H, *J* = 8.6); 7.55 (t, 1H, *J* = 8.3); 7.32 (d, 2H, 4*J* = 2.5); 7.29 (dd, 2H, 4*J* = 2.5, 3*J* = 8.3); 6.99 (dd, 2H, 3*J* = 8.3, 4*J* = 2.2)); 6.82 (m, 1H, 4*J* = 2.2). MS (MALDI-TOF): *m/z* 363.10 $[M]^+$, calcd. 363.08.

2.4.2. 4,4′-[1,4-Phenylenebis(oxy)]diphthalonitrile (**3**)

Yield: 0.79 g (76%) mp 190 °C. FT-IR: ν_{max}, cm^{-1} 3085, 2921, 2852 (C_{ar}–H); 2233 (C≡N); 1587, 1479 (C_{ar}=C_{ar}); 1249 (Ar–O–Ar). ^{1}H NMR (500 MHz, $CDCl_3$): δ, ppm 8.01 (d, 2H, *J* = 8.7); 7.64 (d, 2H, *J* = 2.5); 7.48 (dd, 2H, *J* = 8.7, 2.6); 7.35 (s, 4H). MS (MALDI-TOF): *m/z* 363.09 $[M]^+$, calcd. 363.08.

2.5. Synthesis of Magnesium Tetrakisdicyanophenoxyphenoxyphthalocyaninates

Phenylenebisoxydiphthlonitrile (**2** or **3**) (0.15 g, 0.41 mmol) and anhydrous magnesium acetate were poured into a ceramic crucible and then heated at 190 °C for 30 min in the absence of solvent. After the melt solidified, the mixture was cooled to room temperature, filtered with a Schott filter, and washed with chloroform. The solvent was distilled off, and the filtrate was purified using column chromatography (silica gel M60, chloroform–ethanol (0 to 5 vol.%) gradient) and gel permeation chromatography (2.5% ethanol in chloroform). The complexes were obtained as a dark green powder, soluble in most organic solvents ($CHCl_3$, DMF, DMSO, THF, etc.).

2.5.1. Mg(II) Tetrakis-4-[3-(3,4-dicyanophenoxy)phenoxy]phthalocyaninate (**4**)

Yield: 0.065 g (32%). El. analysis (%): calcd. for ($C_{88}H_{40}MgN_{16}O_8$) C 71.72, H 2.74, N 15.21, O 8.69; found C 71.72, H 2.74, N 15.21, O 8.69. FT-IR: ν_{max}, cm^{-1} 3072, 2919, 2851 (C_{ar}–H); 2234 (C≡N); 1584, 1473 (C_{ar}=C_{ar}); 1241 (Ar–O–Ar). ^{1}H NMR (500 MHz, DMSO-d_6): δ, ppm 7.88 (s, 2H); 7.87 (s, 2H); 7.50 (t, *J* = 8.5 Hz 1H); 7.38 (dd, *J* = 8.4 Hz, 1H); 7.36 (dd, *J* = 8.4 Hz, 1H); 7.02 (dd, *J* = 8.4 Hz, 1H); 7.00 (dd, *J* = 8.4 Hz, 1H); 6.96 (s, 1H). MS (MALDI-TOF): *m/z* 1474.63 $[M + H]^+$, calcd. 1473.64.

2.5.2. Mg(II) Tetrakis-4-[4-(3,4-dicyanophenoxy)phenoxy]phthalocyaninate (**5**)

Yield: 0.053 g (26%). El. analysis (%): calcd. for ($C_{88}H_{40}MgN_{16}O_8$) C 71.72, H 2.74, N 15.21, O 8.69; found C 71.71, H 2.74, N 15.21, O 8.70. FT-IR: ν_{max}, cm^{-1} 3073, 2918, 2852 (C_{ar}–H); 2232 (C≡N); 1590, 1476 (C_{ar}=C_{ar}); 1234 (Ar–O–Ar). ^{1}H NMR (500 MHz, $CDCl_3$): δ, ppm 7.82 (s, 4H); 7.80 (s, 4H); 7.37 (d, *J* = 8.1 Hz, 8H); 7.35 (d, *J* = 2.4 Hz 4H); 7.33 (d, *J* = 2.5 Hz 4H); 7.28 (s, 16H). MS (MALDI-TOF): *m/z* 1474.83 $[M + H]^+$, calcd. 1473.81.

2.6. Synthesis of Metal-Free Tetrakis-4-[3,4-dicyanophenoxyphenoxyphthalocyanines

Compounds **4** and **5** (0.05 g. 0.03 mmol) were dissolved in a molar excess of concentrated (33%) hydrochloric acid (24.50 mL, 0.15 mmol) upon complete dissolution (about 20 min). The acids were distilled, and the final precipitates were washed with water until reaching a neutral pH. Final metal-free phthalocyanines presented as a blue powder, with solubility characteristics similar to those of **4** and **5**.

2.6.1. Tetrakis-4-[3-(3,4-dicyanophenoxy)phenoxy]phthalocyanine (**6**)

Yield: 0.014 g (21%). El. analysis (%): calcd. for ($C_{88}H_{42}N_{16}O_8$) C 72.82, H 2.92, N 15.44, O 8.82; found C 72.81, H 2.90, N 15.47, O 8.82. FT-IR: ν_{max}, cm^{-1} 3079, 2920, 2851 (C_{ar}–H); 2231 (C≡N); 1584, 1475 (C_{ar}=C_{ar}); 1240 (Ar–O–Ar). ^{1}H NMR (500 MHz, $CDCl_3$): δ, ppm 7.82 (s, 2H); 7.80 (s, 2H); 7.58 (t, *J* = 8.2 Hz, 1H); 7.39 (s, 1H); 7.37 (dd, *J* = 8.2 Hz, 1H); 7.35 (dd, *J* = 8.2 Hz, 1H); 7.33 (dd, *J* = 8.2 Hz, 1H); 7.05 (dd, *J* = 8.3 Hz, 2H); 7.03 (dd, *J* = 8.3 Hz, 2H). MS (MALDI-TOF): *m/z* 1451.38 $[M]^+$, calcd. 1451.38.

2.6.2. Tetrakis-4-[4-(3,4-dicyanophenoxy)phenoxy]phthalocyanine (**7**)

Yield: 0.014 g (18%). El. analysis (%): calcd. for ($C_{88}H_{42}N_{16}O_8$) C 72.82, H 2.92, N 15.44, O 8.82; found C 72.80, H 2.91, N 15.45, O 8.84. FT-IR: ν_{max}, cm^{-1} 3077, 2917, 2850 (C_{ar}–H); 2233 (C≡N); 1596, 1481 (C_{ar}=C_{ar}); 1243 (Ar–O–Ar). ^{1}H NMR (500 MHz, $CDCl_3$): δ, ppm 7.81 (s, 4H); 7.79 (s, 4H); 7.26 (d, *J* = 2.6 Hz, 8H); 7.21 (d, *J* = 2.5 Hz, 4H); 7.19 (d, *J* = 2.5 Hz, 4H); 7.08 (s, 16H). MS (MALDI-TOF): *m/z* 1451.39 $[M]^+$, calcd. 1451.38.

(Note: all the spectra are provided in the Supplementary Materials).

3. Results and Discussion

3.1. Synthesis and Characterization

In the initial stage, the goal was to obtain substituted precursors for the synthesis of phthalocyanines and their complexes. Phthalic acids, phthalodinitriles, phthalimides, and diimine benzoindolines are usually used as such compounds. As we showed earlier [23], the tetramerization reaction of phthalodinitriles with cyano groups in absence of solvent leads to the formation of a phthalocyanine macroring withhigh yields. In addition, phthalodinitriles do not require the addition of nitrogen-donor compounds, which could lead to side processes.

It is known that unsubstituted phthalocyanines are practically insoluble in most solvents. To impart solubility to the peripheral and non-peripheral fragments, appropriate substituents are introduced. In this work, [3/4-(3,4-dicyanophenoxy)phenoxy substituents were introduced into the peripheral fragments of the macrocycle molecule. Aryl fragments impart good solubility to structures in organic solvents, and their connection through flexible oxygen bridges improves the mobility of the fragments, thereby leveling the bulkiness of the aromatic rings and preventing aggregation. Cyano groups in combination with oxygen

atoms decrease the electron density from the macrocycle to the periphery, thereby reducing the fluorescence intensity of the molecules. 4,4′-[1,4-phenylenbis(oxy)]diphthalonitrile and 4,4′-[1,3-phenylenbis(oxy)]diphthalonitrile were synthesized by the nucleophilic replacement of the 4-nitrophthalonitrile's (**1**) nitro group with corresponding isomers of dihydroxybenzene (Scheme 1*i*), according to [23].

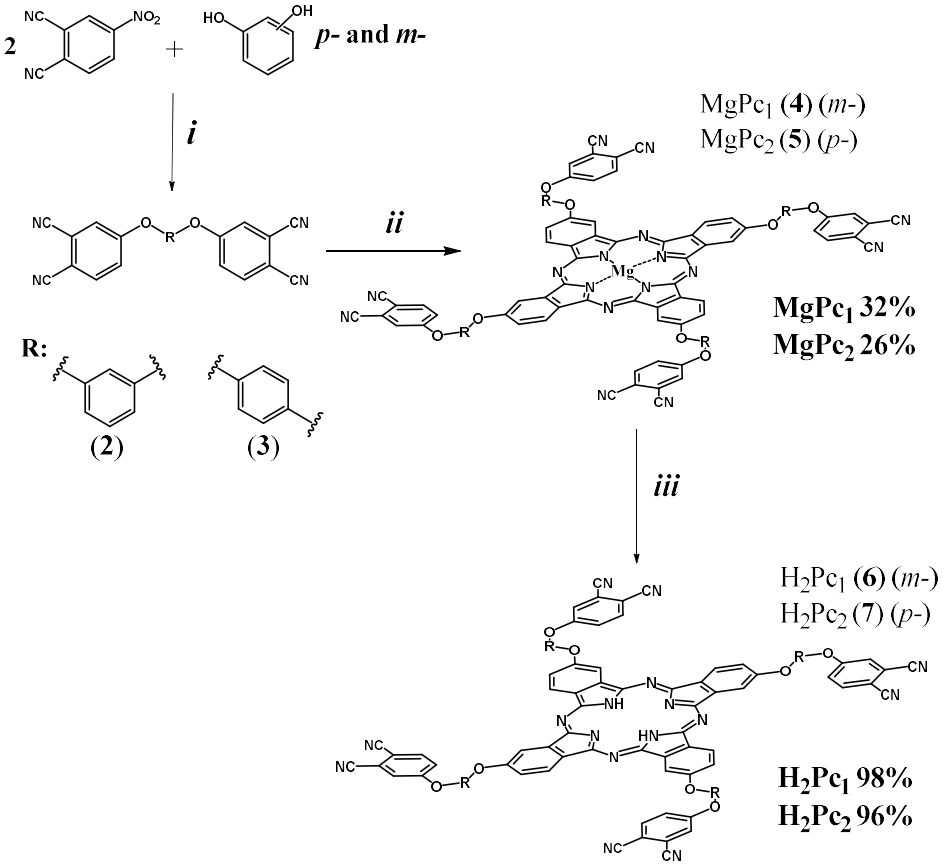

Scheme 1. General synthetic route for obtaining substituted phthalodinitriles **2**–**3** and phthalocyanines **4**–**7**. (***i***) K_2CO_3, DMF, 153 °C, 8 h; (***ii***) $MgAc_2$, 190 °C, 30 min; (***iii***) HCl, refluxing for 20 min.

The structures of compounds **2** and **3** were confirmed using NMR, IR, electron absorption spectroscopy, mass spectrometry, and elemental analysis (See Supplementary Materials for details).

The synthesis of phthalocyanines and their complexes is carried out in several ways. The most common method is tetramerization in a high-boiling-point solvent in the presence of an organic base. Thus, attempts were made to obtain phthalocyanines in *iso*-amyl alcohol, octanol, and quinoline by boiling for 12 h. However, the target compound was not detected from the mass spectra of the mixture measured every 30 min, and the samples taken did not dissolve in chloroform, acetone, or tetrahydrofuran. This was probably associated with the presence of eight cyano groups available for modification in the structure of the target object and their high activity. Varying the temperature, time, and component ratios yielded no results. Therefore, we decided to synthesize phthalocyanines by means of template fusion in the absence of a solvent, which is known to be a more difficult method.

The synthesis of the phthalocyaninates was carried out by the template melting technique utilizing corresponding nitrile and tetrahydrate acetate of magnesium under a temperature of 190–195 °C for 30 min (Scheme 1*ii*).

It should be noted that in addition to the target phthalocyaninate, side products were also formed in the reaction mass (Scheme S1). Thus, using MALDI-TOF mass spectrometry (Figure S20), the presence of clam-shell-type phthalocyaninates in the reaction mass was shown. However, the number of structures of this type that were formed was extremely

small, so the compounds were not purposefully isolated. In addition, at the filtration stage, dark green precipitates that were insoluble in organic solvents were released, which were presumably linear-network polymeric structures of the phthalocyanine type.

The obtained mixture, after cooling, was placed back onto the Shott filter and washed with water and ethanol in order to remove the traces of salt and nitrile. Chloroform was applied in order to extract the desired compound and separate it from the polyphthalocyanine fractions. Then, the solvent was removed, and the complex was purified by means of column chromatography (SiO_2), utilizing chloroform as the eluent and gradually adding ethanol at an amount of 0 to 5 vol.%. During the chromatography in the SiO_2-$CHCl_3$ system, the convergence of a yellow-brown fraction was observed, presumably corresponding to unreacted bisphthalonitrile, as well as phthalimide derivatives formed from it during the reaction and other structure types. The green fraction was collected with the addition of 2.5 vol.% ethanol, while at 5 vol.%, a dark green fraction was obtained. By analyzing the fractions using MALDI-TOF mass spectrometry, we found that the second fraction corresponded to the target product, while the third fraction mainly consisted of clam-shell phthalocyaninate as well as oligomeric structures.

The metal-free complexes were obtained by boiling compounds **6**–**7** in concentrated HCl (Scheme 1*iii*). After the demetallation, the reaction mass was precipitated on a mixture of ice with NaCl, filtered, and washed to reach a neutral pH; after this, it was purified by chromatography on silica gel, with chloroform as the eluent. The compounds appeared as blue powders and were obtained in yields close to quantitative (98 and 96%, respectively).

Compounds **4**–**7** were identified using IR and NMR spectroscopy, as well as MALDI-TOF spectrometry. All obtained complexes produced representative molecular signals in the mass spectra, while the signals of the di- and poly-phthalocyanine systems were absent. The corresponding IR spectra for **4**–**7** represented the whole set of characteristic bands. The ^{1}H NMR spectra of the obtained complexes showed no extraneous signals (see Supplementary Materials for details).

3.2. Spectroscopic Properties of Phthalocyaninates

Due to the presence of an extended conjugated aromatic contour in phthalocyanines, these compounds exhibit the intense absorption of light in the visible region. This means that electronic absorption spectroscopy is a simple and fast method for analyzing the properties of these compounds. The electronic absorption spectrum of phthalocyanines presents an intense band (called the *Q* band) in the 600–700 nm region, which is responsible for the purely electronic π-π^* transition, and bands in the near ultraviolet region (*B* bands), which are related to deeper electronic transitions [26]. Symmetrically substituted phthalocyanine ligands have D_{2h} symmetry and are represented by a bifurcated *Q* band, which merges into a single band during the formation of a complex, accompanied by an increase in symmetry to D_{4h}. When side processes, such as aggregation, occur in solutions, changes in the nature of the spectral curve are observed: for example, a change in the ratio of the intensities of the two main absorption bands, the broadening of the *Q* band, and the appearance of new bands in the spectrum.

During the first stage of studying the spectroscopic properties of the obtained compounds, their characteristics were analyzed in various organic solvents (Table 1). Varying the solvent did not affect the shape of the metal complexes' spectra, but the *Q* band shifted bathochromically or hypsochromically (Figure 1).

The most significant red shift in the band for Pcs was observed in chloroform. This was explained, on the one hand, by the fact that chloroform having the lowest polarity of the studied solvents, and, on the other hand, by its low coordination ability, which led to the relative freedom of the coordination center of the molecules. The *para*-substituted complexes showed a slight bathochromic shift (~1 nm) with respect to the *meta*-analogs. However, the values of the extinction coefficients (and hence the intensity of light absorption) turned out to be higher in the case of meta-substituted phthalocyanines, by 5–7%.

Table 1. Spectroscopic characteristics of phthalocyanines **4**–**7** in different solvents.

Sample	$CHCl_3$			Acetone			DMF		
	λ_{max}^{abs}, nm (lg ε)	λ_{max}^{em}, nm	Stokes Shift, nm	λ_{max}^{abs}, nm (lg ε)	λ_{max}^{em}, nm	Stokes Shift, nm	λ_{max}^{abs}, nm (lg ε)	λ_{max}^{em}, nm	Stokes Shift, nm
4	680 (4.59)	689	9	674 (4.81)	684	10	677 (4.77)	687	10
5	681 (4.34)	693	12	674 (4.43)	683	9	678 (4.55)	689	11
6	664, 700 (3.95)	707	7	661, 694 (3.96)	702	8	667, 699 (3.97)	702	3
7	665, 701 (3.91)	707	6	662, 695 (3.95)	703	8	677, 700 (3.97)	703	3

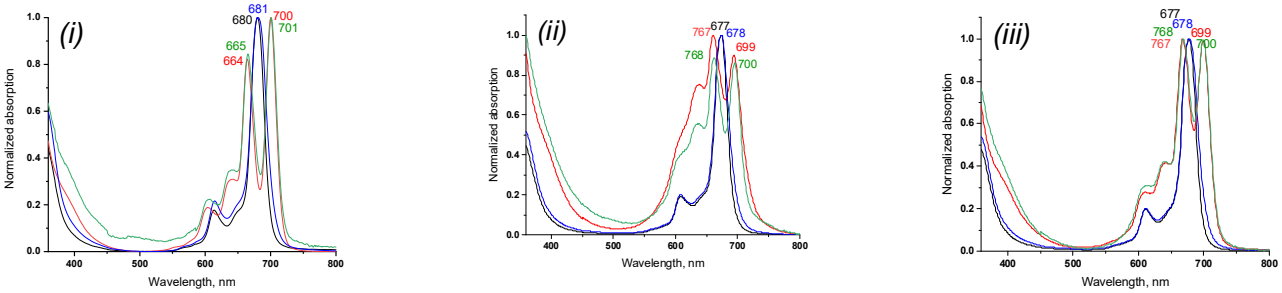

Figure 1. Normalized UV-vis spectra of complexes **4** (black curve), **5** (blue curve), **6** (red curve), and **7** (green curve) in $CHCl_3$ (***i***), acetone (***ii***), and DMF (***iii***).

3.3. Aggregation Studies

Aggregation is an important phenomenon in phthalocyanine chemistry. Phthalocyanines in the aggregated state have different properties from non-aggregated phthalocyanines. Phthalocyanines are characterized by two types of aggregation, *J* and *H* [32,33]. In general, while aggregation decreases the intensity of the *Q* band, it increased the intensity of a new, broader and blue-shifted or red-shifted band. *H* aggregation is visible at smaller wavelength shifts in Pcs, whereas *J* aggregation, corresponding to a red shift, has a larger wavelength shift and is rarely found in phthalocyanines. The aggregation behavior of the synthesized compounds was determined using electron spectroscopy and studied in various solvents, i.e., chloroform, acetone, and dimethylformamide. When compounds **4-5** were diluted, practically no deviations from the linear dependence were observed, which indicated the absence of aggregation in these compounds (Figure 2).

There were no deviations from the Lambert–Bouguer–Beer law observed upon studying the concentration dependence for solutions of the phthalocyaninates in chloroform, acetone, or DMF, which was due to the specific solvation of the central metal cation by these solvents (Figure 1).

One can conclude that the macrocyclic chromophore of the complexes studied under these conditions remained constant. Based on the absence of red or blue shifts in the *Q* band, as well as the linearity of the dependence of the change in optical density on concentration (insertions in Figure 1), it can be concluded that in the studied concentration range, the chromophore existed in the monomeric state.

Compounds **6**–**7** in chloroform also showed the linear dependence of concentration on optical density in the studied concentration range, which indicated the absence of any aggregation processes.

In turn, in acetone and DMF, a strong broadening of the absorption spectra of compounds **6**–**7** was observed, which could be associated with aggregation (Figure 3). To explain this phenomenon, the phthalocyanine solutions were diluted in a wide concentration range. As a result, it was shown that with a decrease in the concentration of the compounds, the form of the spectra got changed, specifically, the ratio of the intensity of the *Q* band components and the position of band (the bathochromic shift were observed). The Labmert–Bouguer–Beer curve also displayed non-linear characteristics (insertion in Figure 3), which together may indirectly indicate the presence of *J*-type aggregates in the solution.

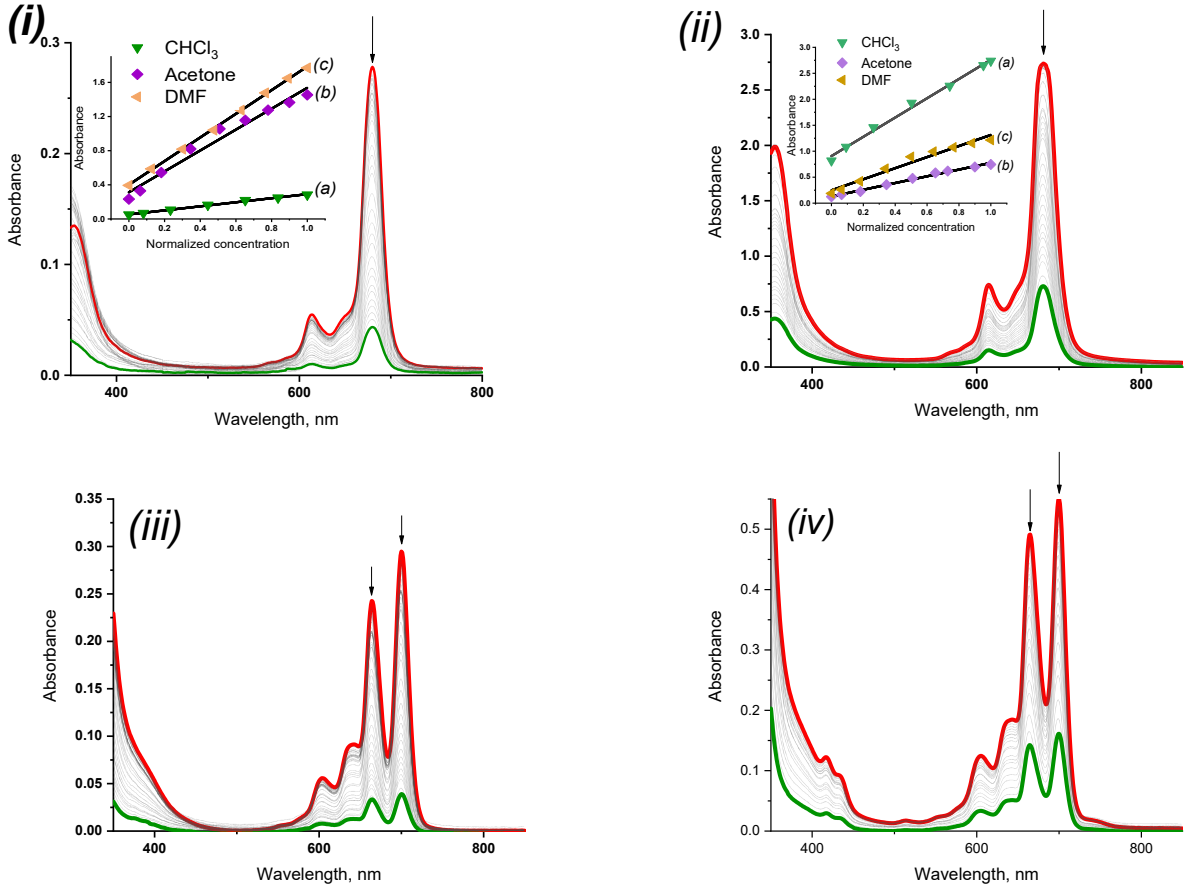

Figure 2. Changes in UV-vis spectra of compound **4** (*i*), **5** (*ii*), **6** (*iii*), and **7** (*iv*) solutions in $CHCl_3$ upon dilution at concentration range of 5.46×10^{-5} mol/L to 1.17×10^{-5} mol/L. Insertion: the Lambert-Buger-Beer dependences in chloroform (*a*), acetone (*b*), and dimethylformamide (*c*) (red curve—initial spectrum; green curve—final spectrum). Note: spectra for compounds in acetone and DMF are provided in Supplementary Materials).

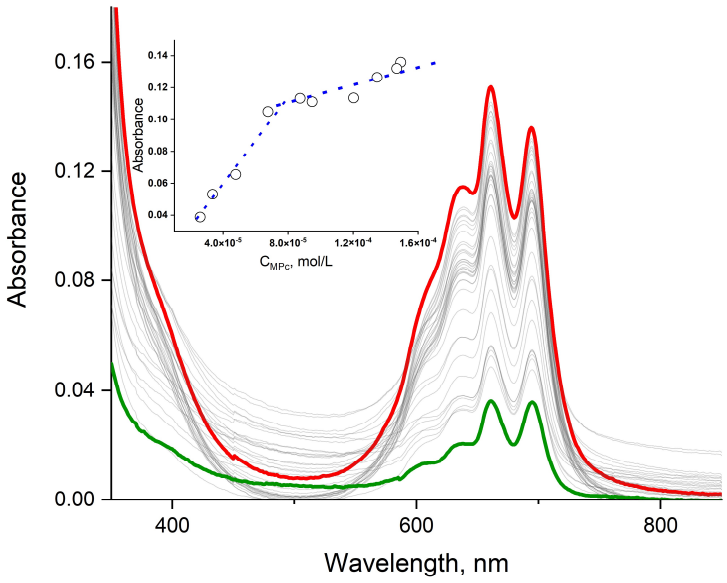

Figure 3. The dilution of compound **6** in acetone solution at the concentration range of $5.58 \times 10^{-6} \div 1.9 \times 10^{-6}$ mol/L (red curve—initial spectrum; green curve—final spectrum).

3.4. Photophysical Studies

3.4.1. Fluorescence Quantum Yields and Lifetimes

The fluorescence quantum yield (Φ_x) and fluorescence lifetime (τ_f) values of the phthalocyanine compounds (**4**–**7**) in chloroform, acetone, and DMF are presented in Table 2.

Table 2. Photophysical values of the synthesized metallated and metal-free phthalocyanines (**4**–**7**) in $CHCl_3$, acetone, and DMF.

Sample	$CHCl_3$			Acetone			DMF			THF
	Φ_x *	τ_f (ns) *	K_{SV}	Φ_x	τF	K_{SV}	Φ_x	τF	K_{SV}	Φ_Δ
4	0.34	5.62	78.36	0.18	5.85	61.99	0.21	5.49	32.15	0.11
5	0.32	5.66	62.15	0.14	5.50	93.71	0.19	5.38	28.44	0.04
6	0.15	6.02	29.84	0.14	6.01	73.65	0.09	4.98	31.32	-
7	0.13	6.03	22.24	0.13	5.93	39.40	0.06	5.25	23.92	-

* The measurement of parameters was carried out at a *Q* band optical density of 0.09 (~2×10^{-6} mol/L) to avoid the concentration quenching of fluorescence.

Fluorescence spectra were recorded upon excitation at the wavelength of the vibrational satellite of the *Q* band (Figure 4). The analysis of the data showed that there was a regular decrease in the fluorescence quantum yields in all the studied solvents when moving from meta-substitution to para-substitution, which was probably due to the greater spatial flexibility of the molecules in the second case. The metal complexes of phthalocyanines exhibited higher fluorescence quantum yields as compared to ligands. This may have been due to the weakening of the universal solvating force of the solvent during the transition from complexes to ligands, as well as the increase in the role of specific solvation.

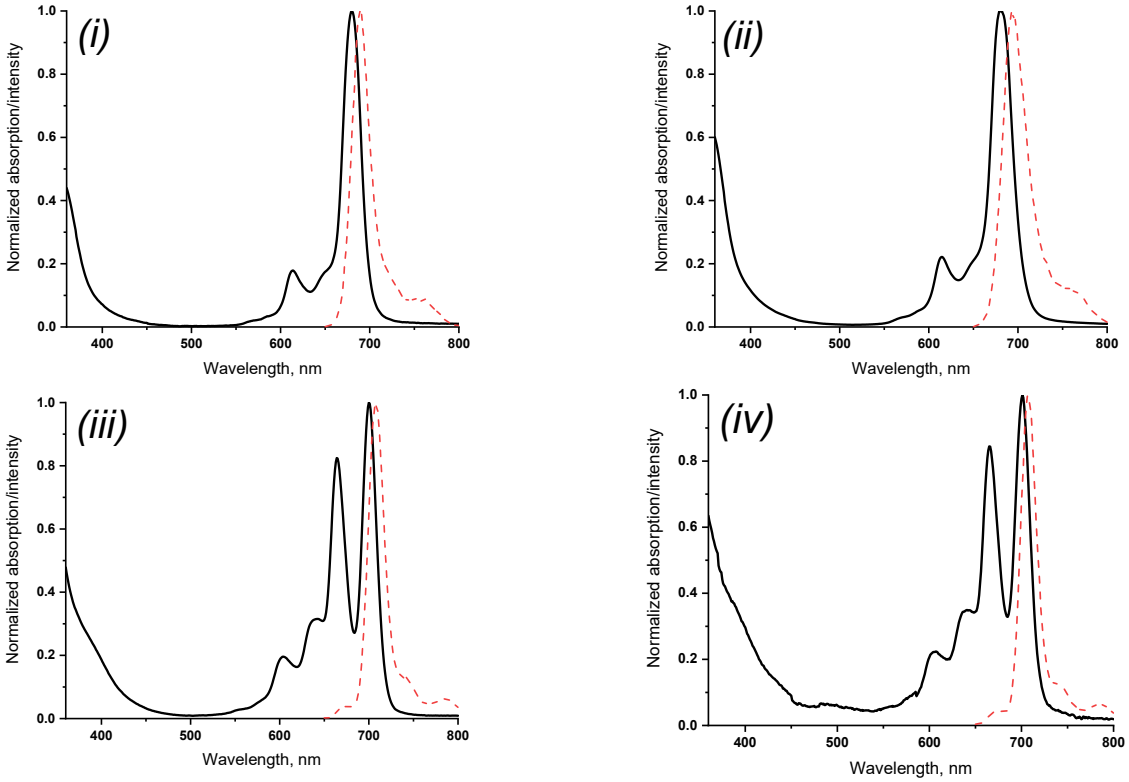

Figure 4. Normalized UV–Vis absorption spectra (black) and fluorescence spectra (dashed red) for compound **4** (*i*), **5** (*ii*), **6** (*iii*), and **7** (*iv*) solutions in $CHCl_3$, sample concentration ~10 μM. For fluorescence measurements, excitation was performed at the absorption maximum of the vibrational satellite (about 610 nm) (note: spectra in acetone and DMF are provided in the Supplementary Materials).

In general, following the series chloroform–acetone–DMF, there was a regular decrease in the fluorescence quantum yields. This could be associated with an increase in the polarity of the medium or with an increase in the coordinating force of the solvents and, consequently, the solvation of the coordination center of the phthalocyanine molecules. A deviation from this dependence was observed only in the case of metal-free phthalocyanines in acetone and DMF. Ligands **6**–**7** in acetone even at low concentrations (~3.51×10^{-6} mol/L) had a broadened *Q* bands, i.e., were in an aggregated state. This explains the increased quantum yields in comparison with chloroform and acetone, which led to a deviation from the described dependence. On the whole, magnesium phthalocyaninates showed a fluorescence quantum yield comparable to unsubstituted ZnPc (0.20), and in chloroform the value was found to be about 50–55% higher.

The data obtained showed that the type of substitution had practically no effect on the fluorescence lifetime (Figure 5), while the presence of a magnesium atom led to a small decrease (~0.10–0.40 ns) in this value. Nevertheless, in general, the fluorescence lifetimes for the studied compounds were found to be 30–39% higher compared to those of unsubstituted zinc phthalocyanine [28], which could be explained by an increase in the energy interval between the basic S_0 and excited S_1 in the substituted phthalocyanine, as compared to the unsubstituted analog. The nature of the metal, as can be seen from the obtained data, did not make a significant contribution to the lifetime values.

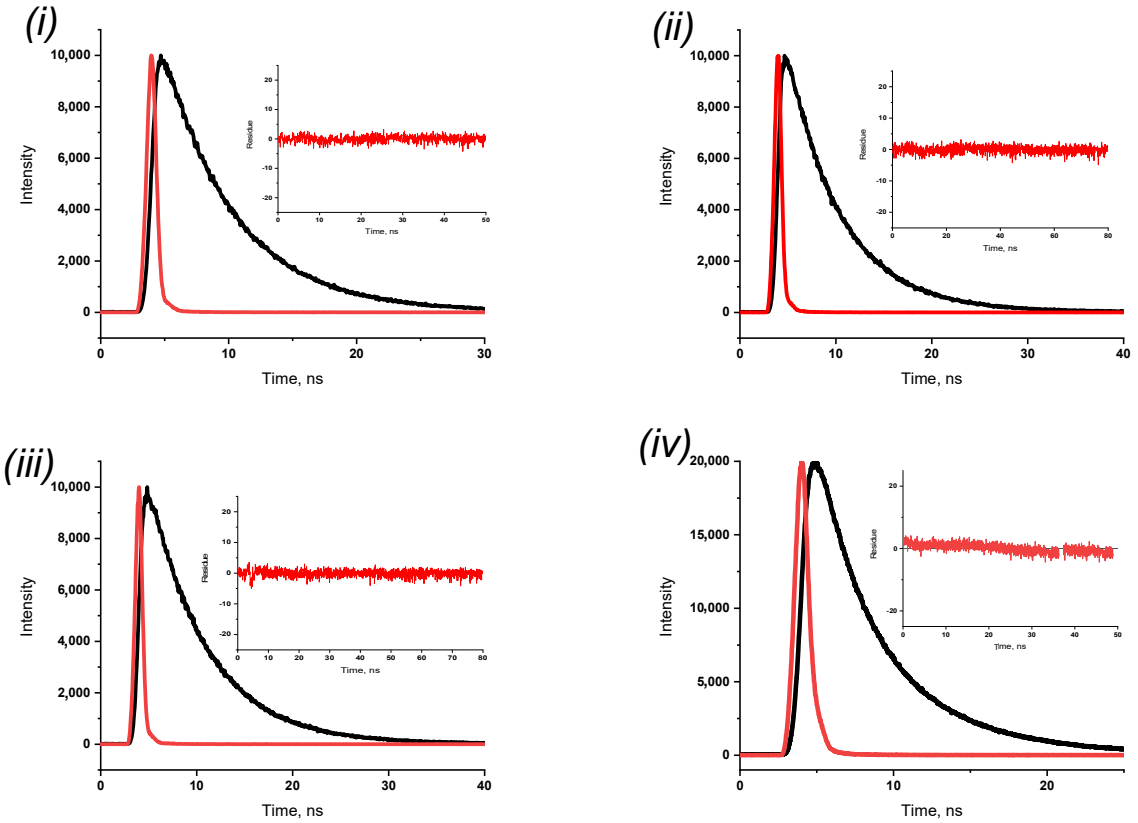

Figure 5. Fluorescence decays with excitation at the absorption maximum of the vibrational satellite for compound **4** (*i*), **5** (*ii*), **6** (*iii*), and **7** (*iv*) solutions in $CHCl_3$, sample concentration ~10 μM (blackcurve—phthalocyanine decay; red curve—LUDOX decay). Data fitting to monoexponential function using deconvolution method, chi-squared value between 1.00 and 1.15 (note: spectra in acetone and DMF are presented in the Supplementary Materials).

3.4.2. Fluorescence Quenching

The fluorescence decay of phthalocyanines **4**–**7** upon the addition of benzoquinone (BQ) in chloroform, acetone, and DMF was found to obey Stern-Volmer kinetics, which was consistent with diffusion-controlled bimolecular reactions [31]. Benzoquinone is frequently

used to determine the fluorescence quenching of phthalocyanine solutions due to its strong affinity for electrons, as well as the high energy of the lowest excited state (higher than the energy of the excited singlet state of metal phthalocyanines), which makes energy transfer from the complex to BQ extremely unlikely.

Figure 6 shows the spectroscopic changes upon benzoquinone addition to phthalocyanine chloroform solutions (changes in acetone and DMF are provided in the Supplementary Materials).

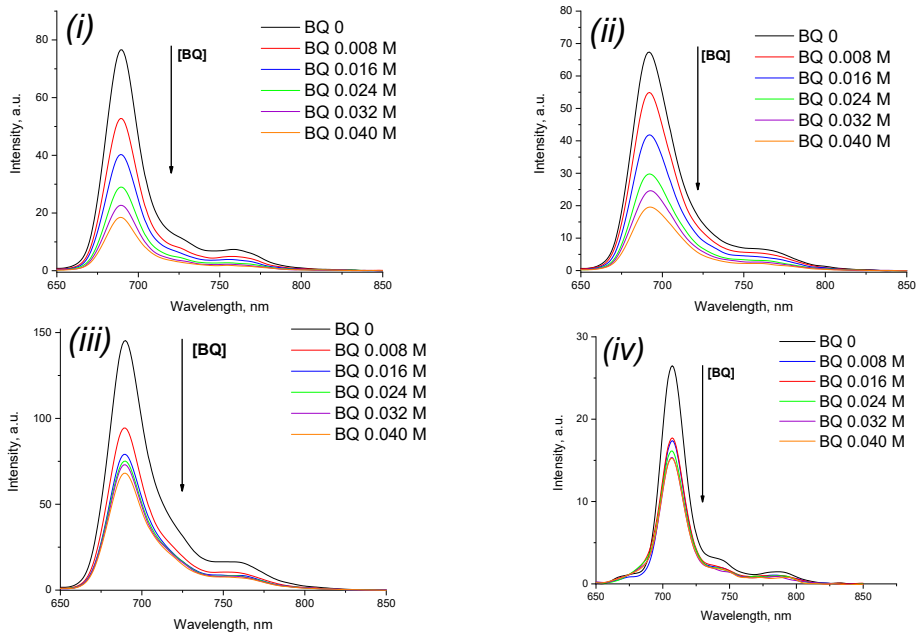

Figure 6. Fluorescence emission spectra changes of **4** (*i*), **5** (*ii*), **6** (*iii*), and **7** (*iv*) upon addition of different concentrations of BQ in $CHCl_3$. BQ = 0, 0.008, 0.016, 0.024, 0.032, 0.040 mol/L (note: spectra in acetone and DMF are presented in the Supplementary Materials).

Based on the data obtained, we determined the dependence of the fluorescence intensity changes of the phthalocyanine solutions in solvents on the concentration of benzoquinone added (Figure 7), which aided in the calculation of the decay constants K_{SV}. The metal complexes showed higher values of the constants compared to the ligands, which was probably associated with the presence of a metal atom in the structure, facilitating the transfer of electrons in excited states from the complex to BQ. In polar DMF, fluorescence quenching proceeded most slowly due to the universal and specific solvation of the molecules' coordination centers being the strongest, which interfered with the described electron transfer process and was found to be even lower than in unsubstituted ZnPc (57.60 in DMF) [34].

3.4.3. Singlet Oxygen Quantum Yield (Φ_Δ) Determination

The main requirement for a sensitizer to be used in PDT is the efficient transfer of energy from its triplet state to molecular oxygen. This process is accompanied by the excitation and generation of its singlet oxygen from molecular oxygen. Thus, the amount of generated singlet oxygen reflects the effectiveness of the compound as a sensitizer. In this work, the ability of the obtained magnesium complexes to generate singlet oxygen was studied as one of the most important characteristics for a photosensitizer. Quantum yields were determined by the chemical trap method using 1,3-diphenylisobenzofuran (DPBF), with unsubstituted zinc phthalocyanine as the standard (Φ_Δ = 0.3 in THF) [35], and the process was monitored using absorption spectroscopy at a wavelength of 415 nm (absorption maximum traps) (Figure 7). During the experiment, a monotonic decrease in the absorption intensity of the trap was observed, caused by its partial destruction under the

action of light, and the intensity of the *Q* band of the sensitizer remained unchanged, which indicated the photostability of the resulting complexes. Schematically, the mechanism of singlet oxygen generation in the presence of phthalocyanine molecules can be represented as follows (Scheme S2) [36]:

$$T_1(Pc) + {}^3O_2 \rightarrow S_0(Pc) + {}^1O_2(\Phi_\Delta) \quad (5)$$

$$DPBF + {}^1O_2(\Phi_\Delta) \rightarrow \text{product type II} \quad (6)$$

where $T_1(Pc)$ is the first triplet Pc state; $S_0(Pc)$ is the ground Pc state; and ${}^1O_2(\Phi_\Delta)$ is singlet oxygen (q.yi.).

The values of the obtained Φ_Δ for compounds **4** and **5** are presented in Table 2. Thus, according to the obtained data, upon the change from para-substitution to meta-substitution in the central benzyl fragment of the peripheral substituent, the quantum yield of singlet oxygen increased almost three-fold.

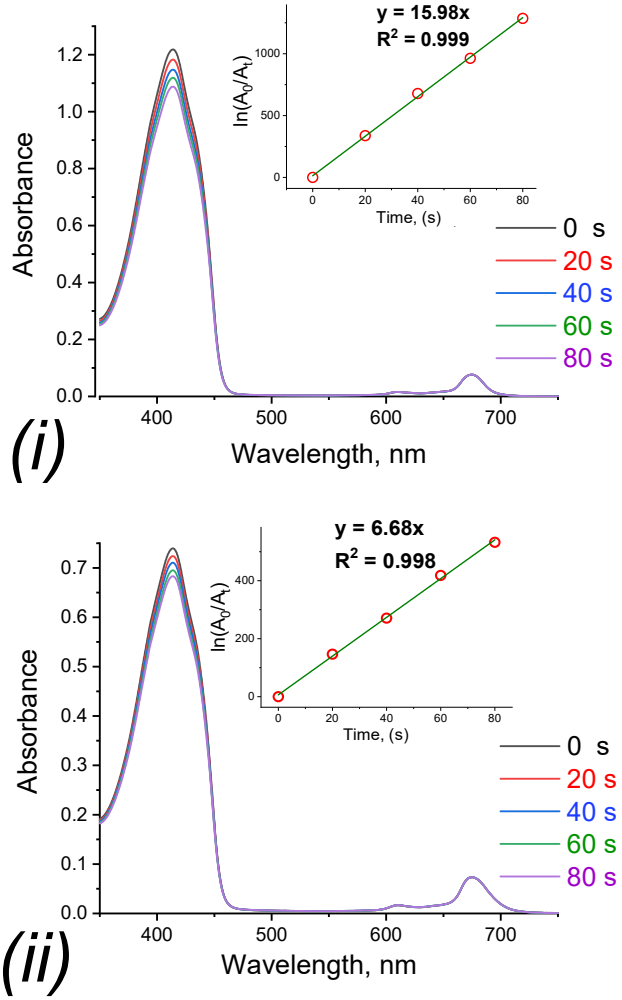

Figure 7. UV-vis absorption spectra changes for **4** (***i***) and **5** (***ii***) in THF upon determination of singlet oxygen quantum yields.

4. Conclusions

Novel peripherally substituted [3/4-(3,4-dicyanophenoxy)phenoxy]phthalocyanines and their complexes with magnesium(II) were synthesized and characterized by NMR, IR, electron absorption spectroscopy, elemental analysis, and mass spectrometry. The compounds showed good solubility in most organic solvents, including chloroform, acetone, and DMF, due to the introduction of suitable substituents, which made it possible to study

their spectroscopic and fluorescent properties in these media. We found that ligands aggregated in acetone and DMF even at relatively low concentrations, while the introduction of magnesium into the coordination center corrected this problem. The metal complexes showed higher extinction coefficients and fluorescence quantum yields in comparison with ligands and unsubstituted zinc phthalocyanine as a standard. It was shown that, in general, the quenching of fluorescence in the studied compounds by the addition of benzoquinone proceeded faster than in cause of unsubstituted ZnPc, and the constants of this process were determined. However, the opposite tendency was observed in the DMF medium. The quantum yields of singlet oxygen were determined for the magnesium complexes, which validated the potential of their use as sensitizers. It was shown that *meta*-substitution in the peripheral substituents led to an increase in the ability to generate singlet oxygen compared to *para*-substitution. In general, the compounds showed good photoactivity and can be used for PDT purposes.

Supplementary Materials: The following supporting information can be downloaded at: https://www.mdpi.com/article/10.3390/chemosensors10120503/s1, Scheme S1: The main reaction products of template tetramerization of substituted phthalonitriles 2 and 3, Figure S1: Changes in UV-vis spectra of compound 4 (i), 5 (ii), and 7 (iii) solutions in acetone upon dilution (note: spectrum for compound 6 is presented in the manuscript), Figure S2: Changes in UV-vis spectra of compound 4 (i), 5 (ii), 6 (iii) and 7 (iv) solutions in DMF upon dilution, Figure S3: Normalized UV–Vis absorption spectra (black) and fluorescence spectra (dashed red) for compound 4 (i), 5 (ii), 6 (iii), and 7 (iv) solutions in acetone, sample concentration ~10 μM. For fluorescence measurements, excitation was performed at the absorption maximum of the vibrational satellite (about 610 nm), Figure S4: Normalized UV–Vis absorption spectra (black) and fluorescence spectra (dashed red) for compound 4 (i), 5 (ii), 6 (iii), and 7 (iv) solutions in DMF, sample concentration ~10 μM. For fluorescence measurements, excitation was performed at the absorption maximum of the vibrational satellite (about 610 nm), Figure S5: Fluorescence decays with excitation at the absorption maximum of the vibrational satellite for compound 4 (i), 5 (ii), 6 (iii), and 7 (iv) solutions in acetone, sample concentration ~10 μM. Data fitting to monoexponential function using deconvolution method, chi-squared value between 1.00 and 1.15, Figure S6: Fluorescence decays with excitation at the absorption maximum of the vibrational satellite for compound 4 (i), 5 (ii), 6 (iii), and 7 (iv) solutions in DMF, sample concentration ~10 μM. Data fitting to monoexponential function using deconvolution method, chi-squared value between 1.00 and 1.15, Figure S7: Stern-Volmer plots for benzoquinone (BQ) quenching of 4–7 in acetone. BQ = 0, 0.008, 0.016, 0.024, 0.032, 0.040 mol/L, Figure S8: Stern-Volmer plots for benzoquinone (BQ) quenching of 4–7 in DMF. BQ = 0, 0.008, 0.016, 0.024, 0.032, 0.040 mol/L, Figure S9: Stern-Volmer plots for benzoquinone (BQ) quenching of 4 (i), 5 (ii), 6 (iii), 7 (iv) in CHCl3. BQ = 0, 0.008, 0.016, 0.024, 0.032, 0.040 mol/L, Figure S10: 1H NMR spectrum of 4 in DMSO-d6, Figure S11: 1H NMR spectrum of 5 in DMSO-d6, Figure S12: 1H NMR spectrum of 6 in DMSO-d6, Figure S13: 1H NMR spectrum of 7 in DMSO-d6, Figure S14: HR MALDI-TOF mass spectrum of 4, Figure S15: HR MALDI-TOF mass spectrum of 5, Figure S16: HR MALDI-TOF mass spectrum of 6, Figure S17: HR MALDI-TOF mass spectrum of 7, Figure S18: Fluorescence emission spectra changes of 4 (i), 5 (ii), 6 (iii), and 7 (iv) upon addition of different concentrations of BQ in DMF. BQ = 0, 0.008, 0.016, 0.024, 0.032, 0.040 mol/L, Figure S19: Fluorescence emission spectra changes of 4 (i), 5 (ii), 6 (iii), and 7 (iv) upon addition of different concentrations of BQ in acetone. BQ = 0, 0.008, 0.016, 0.024, 0.032, 0.040 mol/L, Figure S20: MALDI-TOF mass spectrum of reaction mixture of 4 after template fusion, Scheme S2: Photophysical and photochemical processes involved in photooxidation in the presence of phthalocyanine [36], Figure S21: Plot of $\alpha 2$ versus photon energy of samples 4 (green line), 5 (blue line), and 6 and 7 (red line). The extrapolating light dashed line intersects the value of the optical band gap at the photon energy axis, Table S1: The values of the optical band gap energies (Eg) for phthalocyanines **4**–**7**.

Author Contributions: Conceptualization, D.E. and A.V.; methodology, D.E. and A.V.; software, D.E., S.T. and A.B.; validation, A.V.; formal analysis, D.E. and A.V.; investigation, D.E., S.T. and A.B.; resources, A.V.; data curation, D.E. and A.V.; writing—original draft preparation, D.E.; writing—review and editing, D.E. and A.V.; visualization, D.E., S.T. and A.B.; supervision, A.V.; project administration, A.V.; funding acquisition, A.V. All authors have read and agreed to the published version of the manuscript.

Funding: This research was funded by the Russian Science Foundation, grant number 17-73-20017.

Institutional Review Board Statement: Not applicable.

Informed Consent Statement: Not applicable.

Data Availability Statement: Data available on request.

Conflicts of Interest: The authors declare no conflict of interest.

References

1. Barrett, P.A.; Dent, C.E.; Linstead, R.P. Phthalocyanines. Part VII. Phthalocyanine as a Co-ordinating Group. A General Investigation of the Metallic Derivatives. *J. Chem. Soc.* **1934**, *1936*, 1719–1736. [CrossRef]
2. Kuzmina, E.A.; Dubinina, T.V.; Vasilevsky, P.N.; Saveliev, M.S.; Gerasimenko, A.Y.; Borisova, N.E.; Tomilova, L.G. Novel octabromo-substituted lanthanide(III) phthalocyanines—Prospective compounds for nonlinear optics. *Dye. Pigment.* **2021**, *185*, 108871. [CrossRef]
3. Mutlu, F.; Pişkin, M.; Canpolat, E.; Öztürk, Ö.F. The new zinc(II) phthalocyanine directly conjugated with 4-butylmorpholine units: Synthesis, characterization, thermal, spectroscopic and photophysical properties. *J. Mol. Struct.* **2020**, *1201*, 127169. [CrossRef]
4. De Almeida, R.H.D.; Monroy-Guzmán, F.; Juárez, C.R.A.; Rocha, J.M.; Bustos, E.B. Electrochemical detector based on a modified graphite electrode with phthalocyanine for the elemental analysis of actinides. *Chemosphere* **2021**, *276*, 130114. [CrossRef] [PubMed]
5. Atmaca, G.Y. Measurement of singlet oxygen generation of 9(Hydroxymethyl)anthracene substituted silicon phthalocyanine by sono-photochemical and photochemical studies. *J. Mol. Struct.* **2021**, *1226*, 30–32. [CrossRef]
6. Atmaca, G.Y. Investigation of the differences between sono-photochemical and photochemical studies for singlet oxygen generation of indium phthalocyanine. *Inorg. Chim. Acta* **2021**, *515*, 120052. [CrossRef]
7. Atmaca, G.Y. Investigation of singlet oxygen efficiency of di-axially substituted silicon phthalocyanine with sono-photochemical and photochemical studies. *Polyhedron* **2021**, *193*, 114894. [CrossRef]
8. Orman, E.B.; Sağlam, M.B.; Özkaya, A.R. Novel peripherally substituted metal-free, zinc (II), and cobalt (II) phthalocyanines with 1,1′-thiobis(2-napthol) and additional tetraphthalonitrile groups: Synthesis, aggregation behavior, electrochemical redox and electrocatalytic oxygen reducing prope. *Synth. Met.* **2020**, *263*, 116351. [CrossRef]
9. Silva, N.; Calderón, S.; Páez, M.A.; Oyarzún, M.P.; Koper, M.T.M.; Zagal, J.H. Probing the Fen +/Fe(n − 1)+ redox potential of Fe phthalocyanines and Fe porphyrins as a reactivity descriptor in the electrochemical oxidation of cysteamine. *J. Electroanal. Chem.* **2018**, *819*, 502–510. [CrossRef]
10. Demirbaş, Ü.; Ömeroğlu, İ.; Akçay, H.T.; Durmuş, M.; Kantekin, H. Synthesis, characterization, photophysical and photochemical properties of peripherally tetra benzodioxane substituted metal-free phthalocyanine and its zinc(II) and magnesium(II) derivatives. *J. Mol. Struct.* **2021**, *1223*, 128992. [CrossRef]
11. Yalazan, H.; Köç, M.; Fandaklı, S.; Nas, A.; Durmuş, M.; Kantekin, H. Synthesis, characterization, and photochemical properties of novel peripherally and non-peripherally tetra substituted zinc(II) and magnesium(II) phthalocyanines containing 4-(1,5-diphenyl-4,5-dihydro-1H-pyrazol-3-yl)phenol units. *Polyhedron* **2019**, *170*, 576–583. [CrossRef]
12. Yalazan, H.; Tekintas, K.; Serdaroğlu, V.; Saka, E.T.; Kahriman, N.; Kantekin, H. Design, syntheses, spectroscopic, aggregation properties of novel peripheral octa-substituted zinc(II), magnesium(II) and lead(II) phthalocyanines and investigation of their photocatalytic properties on the photooxidation of 4-nitrophenol. *Inorg. Chem. Commun.* **2020**, *118*, 107998. [CrossRef]
13. Farajzadeh, N.; Kösoğlu, G.; Erdem, M.; Eryürek, G.; Koçak, M.B. Nonlinear optical properties of peripheral symmetrically and non-symmetrically 4-(trifluoromethoxy)phenoxy substituted zinc phthalocyanines. *Synth. Met.* **2020**, *266*, 116440. [CrossRef]
14. Demirbaş, Ü.; Akyüz, D.; Akçay, H.T.; Koca, A.; Menteşe, E.; Kantekin, H. Novel 1,2,4-triazole substituted metallo-phthalocyanines: Synthesis, characterization and investigation of electrochemical and spectroelectrochemical properties. *J. Mol. Struct.* **2018**, *1173*, 205–212. [CrossRef]
15. Biyiklioglu, Z.; Sofuoğlu, A. Peripherally and non-peripherally electropolymerizable (2-{2-[4-(1H-pyrrol-1-yl)phenoxy]ethoxy}ethoxy) group substituted cobalt(II), manganese(III) phthalocyanines: Synthesis and electrochemistry. *J. Mol. Struct.* **2020**, *1212*, 128144. [CrossRef]
16. Akyüz, D.; Demirbaş, Ü.; Akçay, H.T. Synthesis, characterization and electrochemistry of 1-phenoxypropan-2-yloxy substituted phthalocyanines. *J. Organomet. Chem.* **2020**, *923*, 121455. [CrossRef]
17. Vashurin, A.; Maizlish, V.; Kuzmin, I.; Znoyko, S.; Morozova, A.; Razumov, M.; Koifman, O. Symmetrical and difunctional substituted cobalt phthalocyanines with benzoic acids fragments: Synthesis and catalytic activity. *J. Porphyr. Phthalocyanines* **2017**, *21*, 37–47. [CrossRef]
18. Husain, A.; Ganesan, A.; Sebastian, M.; Makhseed, S. Large ultrafast nonlinear optical response and excellent optical limiting behaviour in pyrene-conjugated zinc(II) phthalocyanines at a near-infrared wavelength. *Dye. Pigment.* **2021**, *184*, 108787. [CrossRef]
19. Lobo, C.S.; Tomé, V.A.; Schaberle, F.A.; Calvete, M.J.F.; Pereira, M.M.; Serpa, C.; Arnaut, L.G. Biocompatible ring-deformed indium phthalocyanine label for near-infrared photoacoustic imaging. *Inorg. Chim. Acta* **2021**, *514*, 119993. [CrossRef]

20. Markad, G.B.; Padma, N.; Chadha, R.; Gupta, K.C.; Rajarajan, A.K.; Deb, P.; Kapoor, S. Mutual influence on aggregation and magnetic properties of graphene oxide and copper phthalocyanine through non-covalent, charge transfer interaction. *Appl. Surf. Sci.* **2020**, *505*, 144624. [CrossRef]
21. Berezin, D.B.; Makarov, V.V.; Znoyko, S.A.; Mayzlish, V.E.; Kustov, A.V. Aggregation of water soluble octaanionic phthalocyanines and their photoinactivation antimicrobial effect in vitro. *Mendeleev Commun.* **2020**, *30*, 621–623. [CrossRef]
22. Gök, Y.; Gök, H.Z. Effect of substituent patterns on the aggregation and photophysical properties of novel C2-symmetric diol-based peripherally and non-peripherally zinc phthalocyanines. *J. Mol. Struct.* **2020**, *1206*, 127717. [CrossRef]
23. Vashurin, A.; Erzunov, D.; Kazaryan, K.; Tonkova, S.; Tikhomirova, T.; Filippova, A.; Koifman, O. Synthesis, catalytic, spectroscopic, fluorescent and coordination properties of dicyanophenoxy-substituted phthalocyaninates of d-metals. *Dye. Pigment.* **2020**, *174*, 108018. [CrossRef]
24. Erzunov, D.A.; Vashurin, A.S.; Koifman, O.I. Synthesis and spectral properties of isomers of cobalt tetrakis(dicyanophenoxy)phthal ocyaninate. *Russ. Chem. Bull.* **2018**, *67*, 2250–2252. [CrossRef]
25. Erzunov, D.; Sarvin, I.; Belikova, A.; Vashurin, A. Synthesis and Spectroscopic and Luminescent Properties of Er, Yb and Lu Complexes with Cyano-Substituted Phthalocyanine Ligands. *Molecules* **2022**, *27*, 4050. [CrossRef] [PubMed]
26. Gouterman, M. *The Porphyrins Vol III: Physical Chemistry*; Academic Press: New York, NY, USA, 1978.
27. Fery-Forgues, S.; Lavabre, D. Are fluorescence quantum yields so tricky to measure? A demonstration using familiar stationery products. *J. Chem. Educ.* **1999**, *76*, 1260–1264. [CrossRef]
28. De Boni, L.; Piovesan, E.; Gaffo, L.; Mendonça, C.R. Resonant nonlinear absorption in Zn-phthalocyanines. *J. Phys. Chem. A* **2008**, *112*, 6803–6807. [CrossRef]
29. Wöhrle, D. Polymere aus Nitrilen. *Die Makromol. Chem.* **1972**, *160*, 35–101. [CrossRef]
30. Nemykin, V.N.; Kobayashi, N.; Mytsyk, V.M.; Volkov, S.V. The solid phase, room-temperature synthesis of metal-free and metallophthalocyanines, particularly of 2,3,9,10,16,17,23,24-octacyanophthalocyanines. *Chem. Lett.* **2000**, *29*, 546–547. [CrossRef]
31. Rose, J. *Advanced Physico-Chemical Experiments*; J. Wiley: London, UK, 1964.
32. Gandini, S.C.M.; Yushmanov, V.E.; Borissevitch, I.E.; Tabak, M. Intaraction of the tetra(4-sulfonatophenyl)porphyrin with ionic surfactants: Aggregation and location of micelles. *Langmuir* **1999**, *15*, 6233–6243. [CrossRef]
33. Kasha, M.; Rawls, H.R.; El-Bayoumi, M.A. The exciton model in molecular spectroscopy. *Pure Appl. Chem.* **2009**, *11*, 371–392. [CrossRef]
34. Gmrk, G.; Karaolan, G.K.; Erdomu, A.; Gl, A.; Avcata, U. A novel phthalocyanine conjugated with four salicylideneimino complexes: Photophysics and fluorescence quenching studies. *Dye. Pigment.* **2012**, *95*, 280–289. [CrossRef]
35. Kaestner, L.; Cesson, M.; Kassab, K.; Christensen, T.; Edminsen, P.D.; Cook, M.J.; Chambrier, I.; Cesson, G.J.M. Zinc octa-n-alkyl phthalocyanines in photodynamic therapy: Photophysical properties, accumulation and apoptosis in cell cultures, studies in erythrocytes and topical application to Balb/c mice skin. *Photochem. Photobiol. Sci.* **2003**, *2*, 660. [CrossRef] [PubMed]
36. Zhang, X.-F.; Guo, W. Imidazole Functionalized Magnesium Phthalocyanine Photosensitizer: Modified Photophysics, Singlet Oxygen Generation and Photooxidation Mechanism. *J. Phys. Chem.* **2012**, *116*, 7651–7657. [CrossRef]